

Research Article

The Influence of Deposition Conditions on Structural Properties of PbI₂

Ali M. Mousa¹ and Natheer J. Al-rubaie²

¹ Material Research Unit, Department of Applied Sciences, University of Technology, Baghdad, Iraq

² Ministry of Science and Technology, Iraq

Correspondence should be addressed to Ali M. Mousa, alzuher2000@yahoo.com

Received 17 July 2009; Revised 11 November 2009; Accepted 24 November 2009

Recommended by Hahn Choo

The effect of deposition environment conditions on the electrical and structural properties of deposited PbI₂ layers were studied. The layers were deposited from solution under dark and room light illumination with and without applying magnetic field. XRD, electrical, and photo-electrical properties were measured at room temperature. An increase in the grain size versus the platelet area was noticed. The electrical properties revealed a dependence on deposition conditions. Dark conductivity increases from 1.7×10^{-10} to $5 \times 10^{-9} (\Omega\text{cm})^{-1}$ when deposition was carried out in darkness. A gain factor (the ratio between photoconductivity and dark conductivity) of (23) was obtained. The results indicate that the increase in electrical conductivity is mainly due to the plane 001, where the average number of grain boundaries in this plane sharply decreases when deposition takes place in darkness. On the other hand, the increase in photoconductivity could be due to the decrease in the recombination of free carriers along the grain boundaries.

Copyright © 2009 A. M. Mousa and N. J. Al-rubaie. This is an open access article distributed under the Creative Commons Attribution License, which permits unrestricted use, distribution, and reproduction in any medium, provided the original work is properly cited.

1. Introduction

Lead iodide PbI₂ is a promising compound semiconductor material for X-ray imaging devices [1–4]. It is difficult to grow large crystals of PbI₂ with good uniformity; as a result, they are not well suited for applications such as imaging devices which require large surfaces [5–8]. Using thin polycrystalline layer instead of single crystal wafer is an alternative approach to overcome this difficulty which takes advantage of intrinsic properties of lead iodide [9–12].

Deposition of a layer of PbI₂ polycrystalline from solution is a very comfortable and reliable technique [8–11]; the basic principle requires controlled precipitation on substrate in order to form a layer. Hence, the characterization of electrical and structural properties of such layers is of a great concern both for evaluating their ability to fulfill the requirements needed and for improving their preparation.

Although the application of the external magnetic field during the electrodeposition process has gained a lot of attraction [13, 14], little work is found in the literature on the improvement of the thin film by the application of the external magnetic field during the solution deposition process.

In view of this situation we have investigated the structural and electrical properties dependence of the deposited layer on the deposition conditions (including applying homogeneous external magnetic field, room light illumination, and darkness) in order to understand the transformation accompanying the growth from solution.

2. Sample Preparation

Polycrystalline PbI₂ layers samples were prepared on glass substrates using solution growth by employing PbI₂ powder, prepared in the laboratories without further purification. As checked by X-ray fluorescence, the main residual impurity in the base material is Ag < 4 ppm in weight. The polycrystalline layers were grown by dissolving the powder in deionized water at 100 cc up to the limit of solubility of (4.2 g/L at 100°C) [6]. Then, the solution was slowly cooled down to 20°C, and precipitation of small crystallites occurs rapidly. After evaporation of the excess water, thick layers (typically 3–17 μm thick) were obtained on the glass substrates. Two samples undergo precipitation under the influence of

magnetic field (0.2 T) parallel to the deposition direction, one under room light illumination, and the second in darkness. In order to determine the influence of the magnetic fields on the properties of the deposits, depositions were carried out under a magnetic field. For electrical measurements two graphite electrodes (parallel strips at 5 mm in width, separated by 5 mm) were deposited on the front surface.

3. Structure Properties

The average area of platelet was calculated from the surface photo using optical microscope type (NiKon-Cclipsc/ME 600) equipped with digital camera type (DYM 1200F). For such calculations we chose the largest platelet and eight points on the contour. This step was repeated four times. The structural properties of the layers were investigated using X-ray diffraction system (Lab X-XRD-6000/Shimadzu) which has the following characteristics: source: radiation of $\text{CuK}\alpha$ and with wavelength 1.54 Å, scanning speed (5 degree/min), incidence angle 10–60 degree. The interplanar spacing is calculated from diffraction Bragg equation:

$$n\lambda = 2d \sin \theta, \quad (1)$$

where n is a positive integer. d is the interplanar spacing. The average grain size is deduced from Scherrer equation:

$$G.Z = \frac{0.9\lambda}{B \cos \theta}, \quad (2)$$

where λ is the wavelength of X-ray radiation, and B is the full width half max. (FWHM). θ is Bragg diffraction angle. The average number of grain boundaries (N) is calculated from the interelectrode distance (L) and the average grain size ($G.Z$):

$$N = \left(\frac{L}{G.Z} \right) - 1. \quad (3)$$

4. Electrical Conductivity

The electrical resistivity (ρ) of the deposited films is determined as

$$\rho = R \frac{bd}{l}, \quad (4)$$

where l , b , and d are the length, width, and thickness of the film respectively. Sample resistivity was measured with Keithley (602) electrometer. For photoconductivity the distance between the light source (15 mW/cm²) and samples was set to 100 mm. The samples were mounted on X-Y position head, and measurements with different applied voltages were taken once the maximum responsivity position was reached.

TABLE 1: The average grain area of different PbI_2 films.

samples	Deposition conditions	Average platelets area μm^2
1	Dark without applied magnetic field	180.75
2	Dark with applied magnetic field	78.48
3	light without applied magnetic field	23.11
4	light with applied magnetic field	15.584

5. Results and Discussions

5.1. Reflection Optical Microscopy. The optical micrographs shown in Figures 1(a)–1(d) reveal that the layers are made of hexagonal platelets parallel to the substrate plane. The sizes vary from few micrometers to tens of micrometers.

Table 1 summarizes the calculated platelets area in the pictures. It is clear that deposition in dark gives the largest platelets area while deposition in dark with an applied magnetic field decreases the platelets area. Deposition under normal illumination with and without magnetic field gives the smallest platelets area. The results could be explained by adopting the survivor of the fastest model [15]. According to this model nucleation with various orientations can be formed at the initial stage of the deposition and each nucleus competes to grow but only nuclei having the fastest growth rate survive [16]. The decrease of the platelet area with applying magnetic field is probably due to the opposite direction of the magnetic field lines and the direction of the highest growth rate. It seems that lighting and applying magnetic field could block the lateral growth mode.

5.2. X-Ray Diffraction Analysis. From the X-ray diffractograms the planes orientations were determined. Besides, grain size, number of layers (NL), and microstress (σ_s) of PbI_2 were calculated. Figures 2(a)–2(d) shows the XRD of deposited samples prepared under different conditions. Peaks are observed at $d = 6.95, 3.489, 2.328$, and 1.7447 Å° corresponding to (001), (002), (003), and (004) planes respectively; these results are in good agreement with data achieved by [16, 17], while peaks belonging to (102) and (201) planes mentioned in [18] are missing. The height of the (001) peak decreases with applying magnetic field in both cases. The position of the peaks, that is, the crystallographic orientation of the deposited layer, was not shifted in the four samples during the deposition of the layers. Changing deposition condition caused no additional peaks.

The corresponding data, that is, the interplanar distance, average grain size, number of layers, and microstress are presented in Table 2. The largest grain sizes are those of layers deposited under dark without applying magnetic field. The small grains belong to the sample deposited with light under magnetic field. Decreasing grain size with applying magnetic field was observed during the electrodeposition assisted by applied magnetic fields [19, 20].

The number of deposited layers (NL) under light and magnetic field has the higher value, while sample deposited in dark without magnetic field has the smallest value NL.

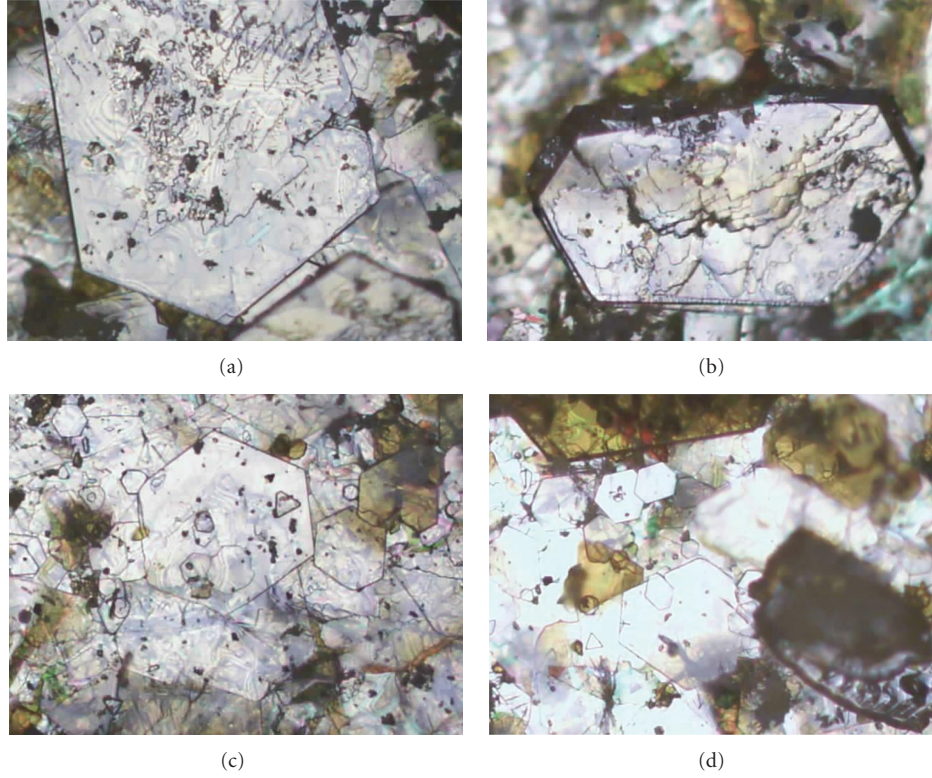


FIGURE 1: Optical micrographs of the PbI_2 films (a) deposited in dark without applied magnetic field, (b) deposited in dark with applied magnetic field, (c) deposited in light without applied magnetic field, and (d) deposited in light with applied magnetic field.

Figures 3(a) and 3(b) show the variation of the grain size with the platelets area for the four growth plans. It is clear that the grain size increases with the increase of platelet area for plane (001) and decreases for (003), (004) plans when the deposition is carried in dark. We think that growth under darkness condition can increase the nucleation frequencies so that nuclei spacing will be small resulting in nuclei growth and coalesce. The principal force behind grain growth is the reduction in the grain boundary surface area per unit volume.

5.3. Electrical Conductivity. Electrical conductivity was calculated from the current-voltage characteristics. Figures 4(a) and 4(b) shows ohmic behavior of both dark and photocurrents for all four samples. By comparing the four curves Figure 4(a) it is concluded that the dark current is higher for the sample deposited in dark with applying magnetic field, while deposition under illumination with and without applying magnetic field gives lower dark current. The low current value for samples deposited under illumination is probably due to the influence of grain boundaries. The grain size was found smaller under illumination; hence the density of their grain boundaries is higher Figure 3(b). This in turn reduces the mobility of charge carriers due to scattering. The influence of grain size is reflected in the photocurrent which in samples (1, 2) is higher than that of samples (3, 4). The increase in the photocurrent is probably due to the reduction of the recombination that takes place in the grain boundaries.

Table 3 shows the variation under dark of the photoconductivity as a function of deposition conditions. The electrical conductivity of samples deposited in darkness is higher than those deposited under light. This could be probably due to the enhancement of the mobilities and the reduction in the grain boundary density.

Figure 5 shows the dark conductivity as a function of the platelet area. The low conductivity belongs to samples deposited under room light illumination. The dependence of conductivity on deposition conditions (see Table 3) has been explained on the basis of inhomogeneous model by Espevik et al. [21]. This model considers the film to consist of conducting grains separated by rather resistive intergranular layers. The conductivity in such films is controlled partially by intergrain barriers with barrier height (E_b). The expression for dark conductivity given by Petriz [22] needs to be modified in our case by adding the intergrain concentration; hence the expression will be

$$\sigma_b \propto \exp\left(-N * \frac{E_b}{kT}\right). \quad (5)$$

Increasing platelet area means increased grain size (decreasing N) and enhanced mobility. However, the reduction in boundary potential in polycrystalline thin film which causes an increase in the carrier concentration cannot be ruled out and therefore it is reasonable to regard this possibility also. The results obtained for the average number of grain

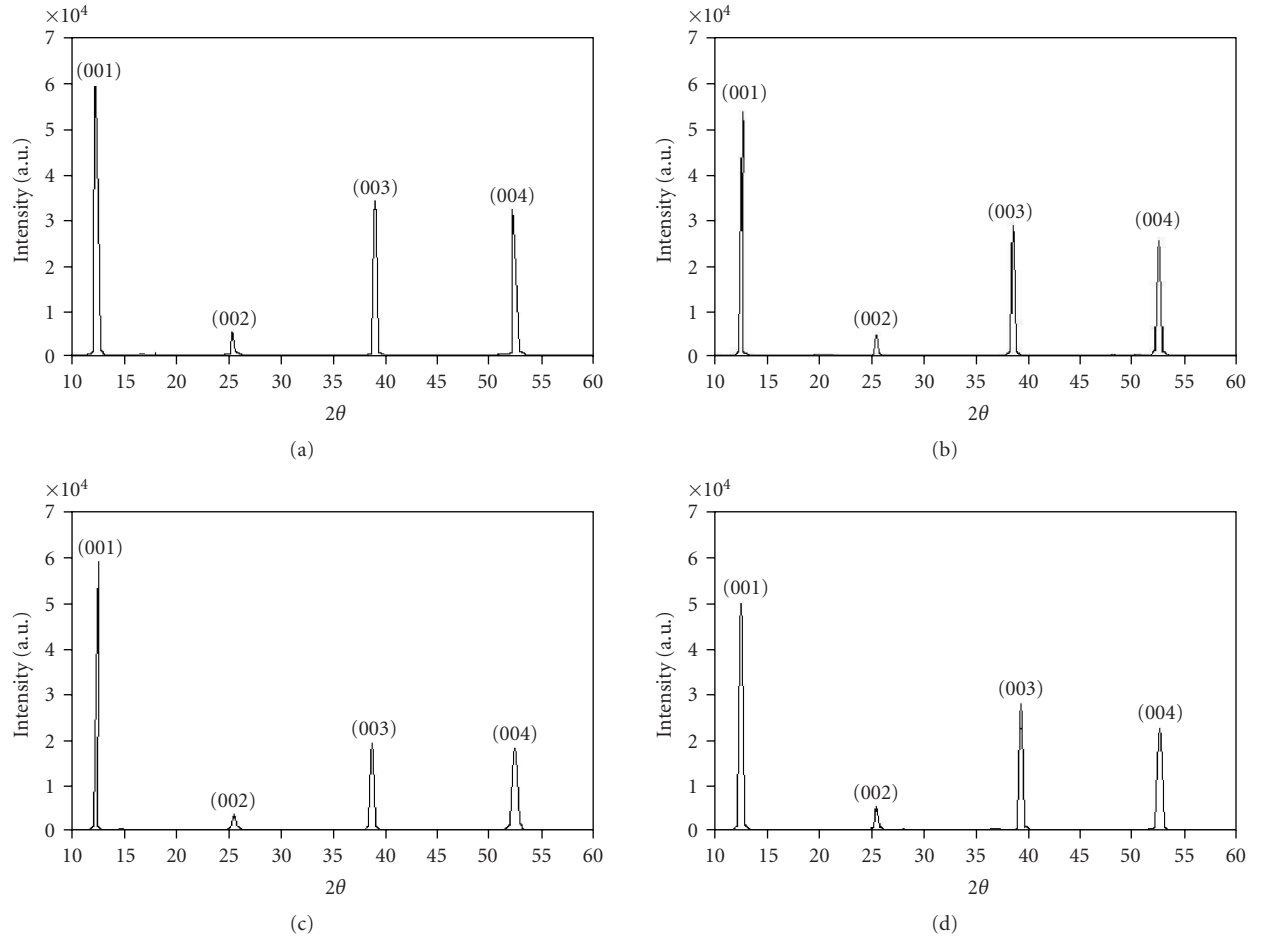


FIGURE 2: XRD patterns for sample deposited in (a) dark without magnetic field, (b) dark with magnetic field, and (c) light without magnetic field, in light with magnetic field.

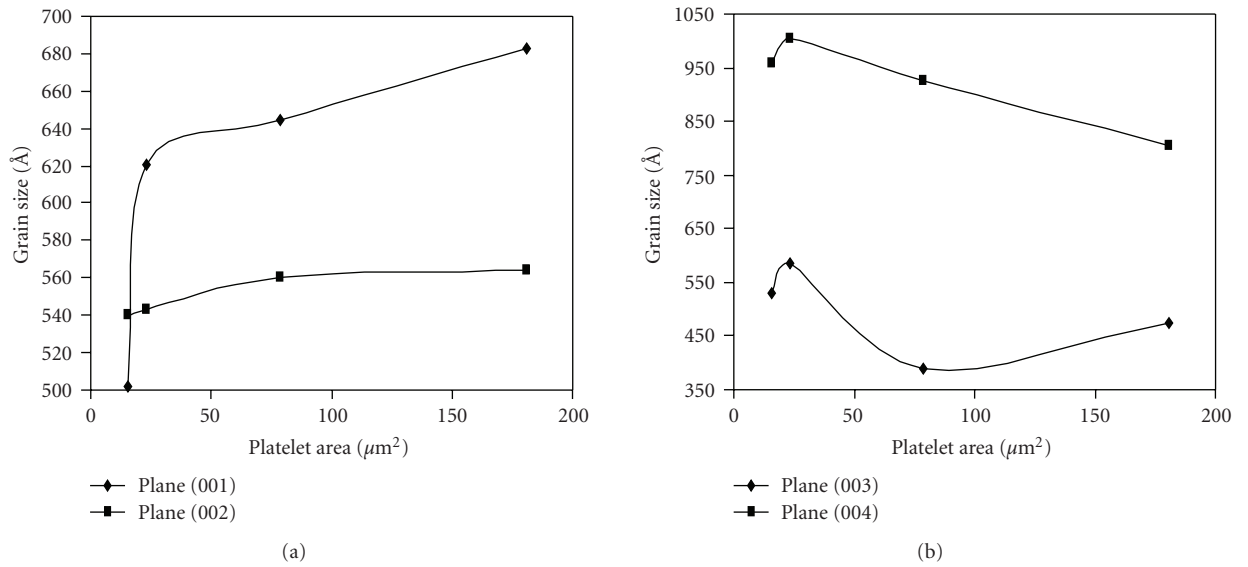


FIGURE 3: The variation in the plane grain size with the platelets area.

TABLE 2: Analysis of the XRD study of undoped PbI₂ films.

Sample	2 θ (degree)	d (Å°)	(hkl)	Grain size Å°	NL
Sample 1	12.7159	6.95896	(001)	682.6201	160
	25.5079	3.48924	(002)	563.7793	206
	38.6427	2.32813	(003)	474.6347	244
	52.3991	1.74474	(004)	805.2267	144
Sample 2	12.732	6.9472	(001)	644.573	164
	25.4861	3.49217	(002)	560.3059	176
	38.6385	2.32838	(003)	390.0919	254
	52.3645	1.74581	(004)	925.2506	107
Sample 3	12.7173	6.9552	(001)	620.2268	161
	25.4451	3.4977	(002)	542.9319	173
	38.5992	2.33066	(003)	585.751	160
	52.3258	1.74701	(004)	1004.105	93
Sample 4	12.7157	6.95607	(001)	501.9222	192
	25.5132	3.48852	(002)	540.2273	178
	38.6713	2.32648	(003)	531.3026	182
	52.3824	1.74526	(004)	958.8356	100

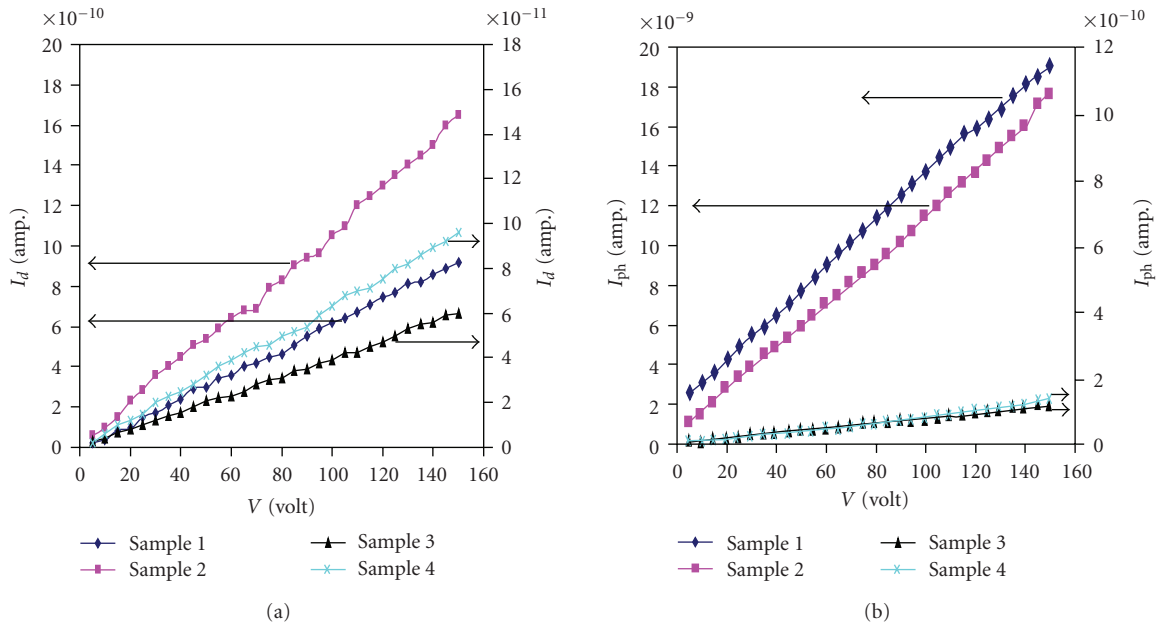


FIGURE 4: Ohmic behavior of both dark and photocurrents of the different samples.

boundary enable us to affirm that the variation in σ_b is mainly due to the 001 plane.

The photoconductivity in PbI₂ layers is due to both direct band-to-band optical transitions and transitions from impurity level (Ag) where both contribute to the creation of electron-hole pairs. The transport of these carriers is determined by the granular structure of the layers and associated trapping centers. $\Delta\sigma/\sigma_d$ ($\Delta\sigma = \sigma_{ph} - \sigma_d$) (optical gain) is a measure of the layers response plotted in Figure 6 as a function of the platelet area. The ratio increases monotonically but nonlinearly; the ratio of sample 1 is higher by a factor of (14) than that of the other three samples.

6. Conclusion

It has been shown that polycrystalline lead iodide layers with interesting structural properties can be prepared by means of a simple solution growth methods. The deposited layers are made of hexagonal platelets parallel to the substrata planes. Their sizes differ from a few micrometers to a tens micrometers. All XRD patterns had the same peaks. Neither on the crystal structure nor on the texture, lighting or magnetic field effect has been observed. All layers irrespective of deposition parameters develop a preferred (001) plane. The grain size increases with the increase of the platelets

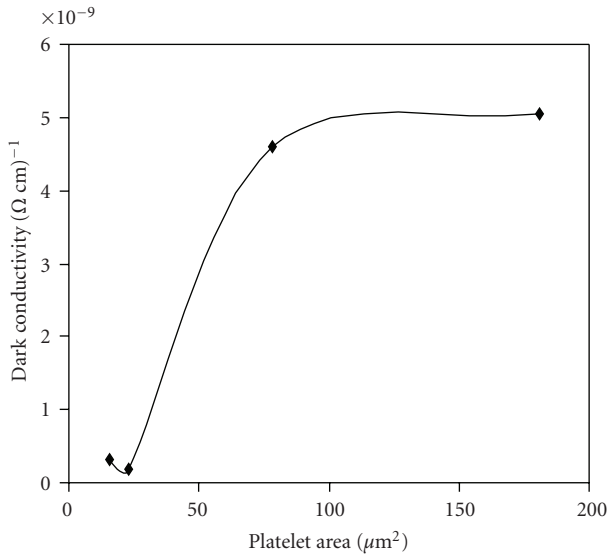


FIGURE 5: Dark conductivity versus platelet area.

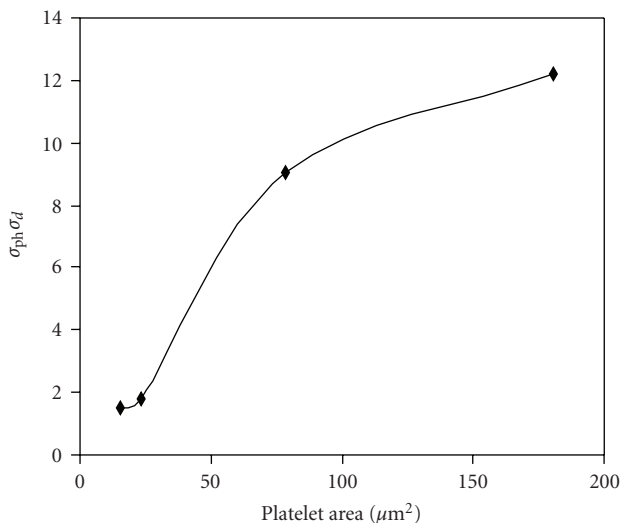


FIGURE 6: Variation in the conductivities versus platelet area.

area when deposition is carried out in darkness (682.6201 A° for platelet area of $180.75 \mu\text{m}^2$, 540.2273 A° for platelet area $15.584 \mu\text{m}^2$). The illumination impact on the chemical reaction rates had strong consequences on the resulting layer characteristics. The most pronounced effect is the electrical characteristics. Dark conductivity increases from 1.7×10^{-10} to $5 \times 10^{-9} (\Omega\text{cm})^{-1}$ when deposition is carried out under darkness. A gain factor (23) was also attained.

References

- [1] A. I. Savchuk, V. I. Fediv, Ye. O. Kandyba, T. A. Savchuk, I. D. Stolyarchuk, and P. I. Nikitin, "Platelet-shaped nanoparticles of PbI_2 and PbMnI_2 embedded in polymer matrix," *Materials Science and Engineering C*, vol. 19, no. 1-2, pp. 59–62, 2002.
- [2] R. A. Street, M. Mulato, M. Schieber, et al., "Comparative study of PbI_2 and HgI_2 as direct detector materials for high resolution X-ray image sensors," in *Medical Imaging: Physics of Medical Imaging*, vol. 4320 of *Proceedings of SPIE*, pp. 1–12, San Diego, Calif, USA, February 2001.
- [3] D. L. Y. Lee, L. K. Cheung, L. S. Jeromin, E. F. Palecki, and B. G. Rodricks, "Radiographic imaging characteristics of a direct conversion detector using selenium and thin film transistor array," in *Medical Imaging: Physics of Medical Imaging*, vol. 3032 of *Proceedings of SPIE*, pp. 88–96, Newport Beach, Calif, USA, February 1997.
- [4] A. I. Savchuk, V. I. Fediv, Ye. O. Kandyba, T. A. Savchuk, I. D. Stolyarchuk, and P. I. Nikitin, "Platelet-shaped nanoparticles of PbI_2 and PbMnI_2 embedded in polymer matrix," *Materials Science and Engineering C*, vol. 19, no. 1-2, pp. 59–62, 2002.
- [5] P. Montgomery, J. Ponpon, M. Sieskind, and C. Draman, "Surface morphology analysis of HgI_2 and PbI_2 with interference microscopy: The challenges of measuring fragile materials and deep surface roughness," *Physica Status Solidi C*, vol. 3, pp. 1044–1050, 2003.
- [6] J. P. Ponpon and M. Amann, "Thermally stimulated current measurements on polycrystalline PbI_2 layers," *The European Physical Journal Applied Physics*, vol. 18, no. 1, pp. 25–31, 2002.
- [7] D. Bahvsar and K. Saraf, "Optical and structural properties of Zn-doped lead iodide thin films," *Materials Chemistry and Physics*, vol. 78, no. 3, pp. 630–636, 2003.
- [8] S. S. Novosad, I. S. Novosad, and I. M. Matviishin, "Luminescence and photosensitivity of PbI_2 crystals," *Inorganic Materials*, vol. 38, no. 10, pp. 1058–1062, 2002.
- [9] A. M. Mousa, "Optical and photoconduction in PbI_2 polycrystalline deposited from solution," *International Journal of Modern Physics B*, vol. 21, no. 21, pp. 3745–3753, 2007.
- [10] J. P. Ponpon, A. M. Mousa, and M. Amann, "Compensation effect of Sn in PbI_2 polycrystalline layers," *Physica Status Solidi A*, vol. 205, no. 7, pp. 1653–1656, 2008.
- [11] M. Yunus, Ph.D. thesis, College of Graduate Studies and Research, University of Saskatchewan, April 2005.
- [12] J. P. Ponpon and M. Amann, "Preliminary characterization of PbI_2 polycrystalline layers deposited from solution for nuclear detector applications," *Thin Solid Films*, vol. 394, no. 1-2, pp. 277–283, 2001.
- [13] A. Krause, M. Uhlemann, A. Gebert, and L. Schultz, "A study of nucleation, growth, texture and phase formation of electrodeposited cobalt layers and the influence of magnetic fields," *Thin Solid Films*, vol. 515, no. 4, pp. 1694–1700, 2006.
- [14] D. Thiemi, C. Kubeil, C. P. Gräf, and A. Bund, "Electrodeposition of magnetic nickel matrix nanocomposites in a static magnetic field," *Thin Solid Films*, vol. 517, no. 5, pp. 1636–1644, 2009.
- [15] A. van der Drift, "Evolutionary selection, a principle governing growth orientation in vapour-deposited layers," *Philips Research Reports*, vol. 22, pp. 267–288, 1967.
- [16] K. Kapoor, D. Lahiri, S. V. R. Rao, T. Sanyal, and B. P. Kashyap, "X-ray diffraction line profile analysis for defect study in Zr-2.5\% Nb material," *Bulletin of Materials Science*, vol. 27, no. 1, pp. 59–67, 2004.
- [17] J. P. Ponpon and M. Amann, "Current instability and polarization phenomena in lead iodide crystalline detectors," *Nuclear Instruments and Methods in Physics Research A*, vol. 526, no. 3, pp. 447–454, 2004.
- [18] V. Deich and M. Roth, "Improved performance lead iodide nuclear radiation detectors," *Nuclear Instruments and Methods in Physics Research A*, vol. 380, no. 1-2, pp. 169–172, 1996.

- [19] I. Tabkovic, S. Riemer, M. Sun, V. A. Vasko, and M. Kief, "Effect of magnetic field on electrode reactions and properties of electrodeposited NiFe films," *Journal of The Electrochemical Society*, vol. 150, pp. C635–C640, 2003.
- [20] I. Tabkovic, S. Riemer, M. Sun, V. A. Vasko, and M. Kief, "Effect of magnetic field on NiCu electrodeposition from citrate plating solution and characterization of deposit," *Journal of The Electrochemical Society*, vol. 152, pp. C851–C860, 2005.
- [21] S. Espevik, C.-H. Wu, and R. H. Bube, "Mechanism of photoconductivity in chemically deposited lead sulfide layers," *Journal of Applied Physics*, vol. 42, no. 9, pp. 3513–3529, 1971.
- [22] R. L. Petritz, "Theory of photoconductivity in semiconductor films," *Physical Review*, vol. 104, no. 6, pp. 1508–1516, 1956.